ORIGINAL ARTICLE

Cancer Science WILEY

ZNF500 abolishes breast cancer proliferation and sensitizes chemotherapy by stabilizing P53 via competing with MDM2

Xiaowen Ma[1,2] | Mingwei Fan[1] | Kaibo Yang[3] | Yuanyuan Wang[4] | Ran Hu[1] | Mengyao Guan[1] | Yuekang Hou[1] | Jiao Ying[1] | Ning Deng[5] | Qingchang Li[1] | Guiyang Jiang[1] | Yong Zhang[6] | Xiupeng Zhang[1]

[1]Department of Pathology, College of Basic Medical Sciences and First Affiliated Hospital of China Medical University, Shenyang, China

[2]Second Department of Clinical Medicine, China Medical University, Shenyang, China

[3]Department of Ophthalmology, The First Hospital of China Medical University, Shenyang, China

[4]Department of Anesthesiology, The Fourth Affiliated Hospital, China Medical University, Shenyang, China

[5]Department of Breast Surgery, Cancer Hospital of China Medical University, Liaoning Cancer Hospital and Institute, Shenyang, China

[6]Department of Pathology, Cancer Hospital of China Medical University, Liaoning Cancer Hospital and Institute, Shenyang, China

Correspondence
Guiyang Jiang and Xiupeng Zhang, China Medical University, No.77 Puhe Road, Shenyang North New Area, Shenyang, Liaoning Province, 110122, China.
Email: gyjiang@cmu.edu.cn and xpzhang@cmu.edu.cn

Yong Zhang, Cancer Hospital of China Medical University, Liaoning Cancer Hospital & Institute, No. 44 Xiaoheyan Road, Dadong District, Shenyang 110042, Liaoning Province, China.
zhangyong@cancerhosp-ln-cmu.com

Funding information
Department of Science and Technology of Liaoning Province, Grant/Award Number: 2020-MS-173

Abstract

Zinc finger protein 500 (ZNF500) has an unknown expression pattern and biological function in human tissues. Our study revealed that the ZNF500 mRNA and protein levels were higher in breast cancer tissues than those in their normal counterparts. However, ZNF500 expression was negatively correlated with advanced TNM stage ($p=0.018$), positive lymph node metastasis ($p=0.014$), and a poor prognosis ($p<0.001$). ZNF500 overexpression abolished in vivo and in vitro breast cancer cell proliferation by activating the p53-p21-E2F4 signaling axis and directly interacting with p53 via its C2H2 domain. This may prevent ubiquitination of p53 in a manner that is competitive to MDM2, thus stabilizing p53. When ZNF500-ΔC2H2 was overexpressed, the suppressed proliferation of breast cancer cells was neutralized in vitro and in vivo. In human breast cancer tissues, ZNF500 expression was positively correlated with p53 ($p=0.022$) and E2F4 ($p=0.004$) expression. ZNF500 expression was significantly lower in patients with Miller/Payne Grade 1–2 than in those with Miller/Payne Grade 3–5 ($p=0.012$). ZNF500 suppresses breast cancer cell proliferation and sensitizes cells to chemotherapy.

KEYWORDS
breast cancer, chemotherapy, MDM2, p53, ZNF500

1 | INTRODUCTION

Breast cancer is the most commonly diagnosed malignant tumor in women.[1] Hormone and targeted therapies achieve better prognoses in some subtypes of breast cancer[2,3]; however, chemotherapy remains the dominant first-line treatment for breast cancer patients. Subsequent chemotherapy resistance is a major issue in improving patient survival time. Therefore, there is an urgent need to characterize the crucial factors that sensitize patients to chemotherapy treatment.

p53 is essential for various cellular processes, such as cell cycle checkpoints,[4] DNA damage repair,[5] and apoptosis.[6] It also plays a pivotal role as a "gatekeeper" in malignancy.[7] However, p53 is often mutated or absent in malignant tumor cells, thus promoting tumor progression.[8,9] Moreover, p53 is an extremely unstable protein with a half-life of 5–30 min.[10] It can be modulated by diverse post-transcriptional modifications, such as phosphorylation,[11] acetylation,[12] and ubiquitination,[13] thus affecting its stability.[14] The MDM2 protein is the most dominant classical E3 ubiquitin ligase, which accelerates p53 nuclear export by promoting its monoubiquitination, followed by its degradation; a process that is dependent on the proteasome.[15]

ZNF500, a member of the C2H2 zinc finger protein family, is localized to the human chromosome 16p13.3. Kupers et al. suggested that ZNF500 is expressed in the subcutaneous adipose tissue of children, but its biological function remains unknown.[16] It consists of a SCAN domain in the N terminus, KRAB domain in the middle, and C2H2 domain in the C terminus, which is responsible for binding to DNA. To date, the expression pattern and biological function of ZNF500 in human tissue, especially malignant tumor tissue, remain unexplored.

2 | MATERIALS AND METHODS

2.1 | Patients and clinical specimens

The study protocol was approved by the Institutional Review Board of China Medical University. All participants provided written informed consent, and the study was performed in accordance with the principles of the Declaration of Helsinki. Detailed descriptions of the information of patients have been previously described[17] and can be found in the Additional file S1.

2.2 | Functional enrichment analyses

As described in the study by Li et al.[18]

2.3 | Western blotting, Proteasome-inhibition and ubiquitination assays and immunoprecipitation

Western blotting and immunoprecipitation were performed as described in the study by Zhang et al.[19] Detailed descriptions of the antibodies are mentioned in the Additional file S1.

2.4 | IHC

IHC analysis was performed as described in a previous study.[20] Detailed descriptions of the antibodies are mentioned in the Additional file S1.

2.5 | Cell culture

Detailed descriptions of the antibodies are mentioned in the Additional file S1.

2.6 | Reagents

Detailed descriptions of the reagents are mentioned in the Additional file S1.

2.7 | MTT and colony formation assay

MTT and colony formation assay were performed as described in the study by Zhang et al.[19]

2.8 | EdU assay and immunofluorescence staining

The assays were performed as described in the study by Zhang et al.[19] The cells were incubated with 20 μM EdU solution (Cellorlab, Shanghai, China) for 1 h, after overexpressing or knocking out ZNF500. Then, the

FIGURE 1 ZNF500 was highly expressed in breast cancer but negatively correlated with poor prognosis. (A) The ZNF500 mRNA level was evaluated among diverse cancer tissue and adjacent tissue according to TCGA. (B) ZNF500 mRNA was detected in breast cancer tissue. (C) Comparison of expression of ZNF500 mRNA in different subtypes of breast cancer. (D) The expression of ZNF500 mRNA was compared between breast cancer patients within NTNBC and TNBC. (E, F) mRNA expression levels of ZNF500 were compared according to Scarff–Bloom Richardson (SBR) and Nottingham prognostic Index (NPI) scores.(G, H) Correlation between ZNF500 mRNA levels and overall survival of patients with breast cancer (I) Comparison of expression of ZNF500 protein in wild-type and mutated P53 in breast cancer patients. (J) ZNF500 protein in 12 freshly isolated samples from patients with breast cancer analyzed by western blotting. (K–N) Representative image of (IHC) staining of ZNF500 in patients with breast cancer. Scale bar, 50 μm. The green enclosure (L) represents enlarged figure for Figure 6K (O) Correlation of ZNF500 protein level with overall survival in patients with breast cancer (P, Q) ZNF500 protein levels and subcellular localization were evaluated by western blotting and IF assays, scale bar = 10 μm. Quantitative data were expressed as mean ± SD of three independent experiments. *$p < 0.05$, **$p < 0.01$, ***$p < 0.001$, t test.
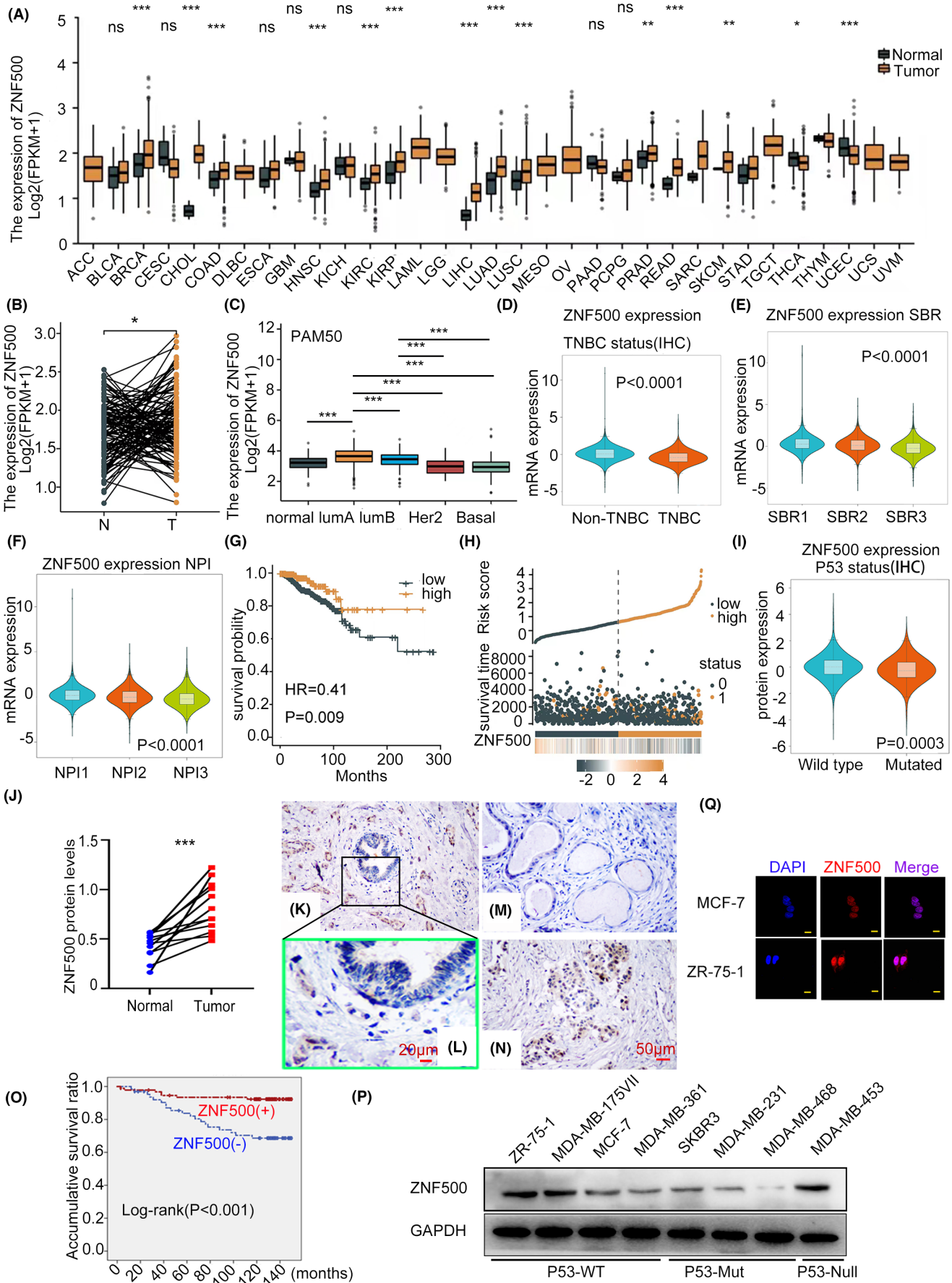
cells were incubated with ZNF500, myc-tag, flag-tag, p53, MDM2, and γ-H2AX antibodies at a concentration ratio of 1:50.

2.9 | Flow cytometry

Flow cytometry was performed as described in the study by Li et al.[18]

2.10 | Transplantation of tumor cells into nude mice

The animals were treated according to the NIH Guidelines for the Care and Use of Laboratory Animals (NIH Publication No. 8023, revised 1978). The nude mice were treated according to the experimental animal ethics guidelines issued at the China Medical University (CMU2021710). Detailed descriptions are mentioned in the Additional file S1.

TABLE 1 Correlation of ZNF500 expression with clinic-pathological features in 157 cases breast cancer.

Clinicopathological factors	N	Positive	Negative	χ^2	p
Age					
<52	86	49	37	0.402	0.625
≥52	69	44	27		
TNM classification					
I+II	99	66	33	6.128	0.018
III	58	27	31		
Lymph node metastasis					
Positive	69	33	36	6.637	0.014
Negative	88	60	28		
Triple negative (ER, PR, Her-2)					
Positive	91	46	45	6.764	0.013
Negative	66	47	19		
P53 status					
Wild-type		50	17	11.466	0.001
Mutant or null		43	47		

TABLE 2 Summary of Cox univariate and multivariate regression analysis of the association between clinicopathological features and overall survival in 157 cases of breast cancer.

Clinicopathological feature	Regression coefficient	Wald chi-squared test	p	Risk ratio	95% CI Lower	Upper
Univariate analysis						
Age	−0.656	2.380	0.123	0.519	0.226	1.194
TNM classification	1.956	17.610	<0.001	7.070	2.836	17.624
Lymph node metastasis	2.174	15.969	<0.001	8.794	3.028	25.544
Triple-negative	0.907	3.792	0.051	2.476	0.994	6.167
P53 status	0.412	0.714	0.398	1.417	0.631	3.179
ZNF500 expression	−1.497	11.440	0.001	0.224	0.094	0.553
Multivariate analysis						
TNM classification	1.759	13.963	<0.001	5.807	2.308	14.612
ZNF500 expression	−1.220	7.444	0.006	0.295	0.123	0.709

FIGURE 2 ZNF500 inhibited tumor proliferation in vitro and in vivo. (A) GSEA analysis was performed to explore the signaling pathway positively correlated with high ZNF500 expression in breast cancer. (B) Overexpression and knockout efficiency ZNF500 was detected by western blotting in MCF-7 or ZR-75-1 cells. (C) MTT, (D) colony formation, (E), EdU assay, scale 50 μm and (F) Flow cytometry assays were assessed to detect the effect of overexpression or knockout of ZNF500 on the proliferation of MCF-7 and ZR-75-1 cells. (G) Cell cycle-related proteins were detected by western blotting after ZNF500 overexpression or knockout in MCF-7 or ZR-75-1 cells. (H) Xenografts assay was performed to investigate the effect on proliferation of MCF-7 cells within overexpression or knockout in vitro. Quantitative data were expressed as mean±SD of three independent experiments. *$p<0.05$, **$p<0.01$, ***$p<0.001$, t test for two groups and one-way ANOVA for multiple groups.

(A) KEGG_CELL_CYCLE

NES=-2.0091
P<2.2e-16
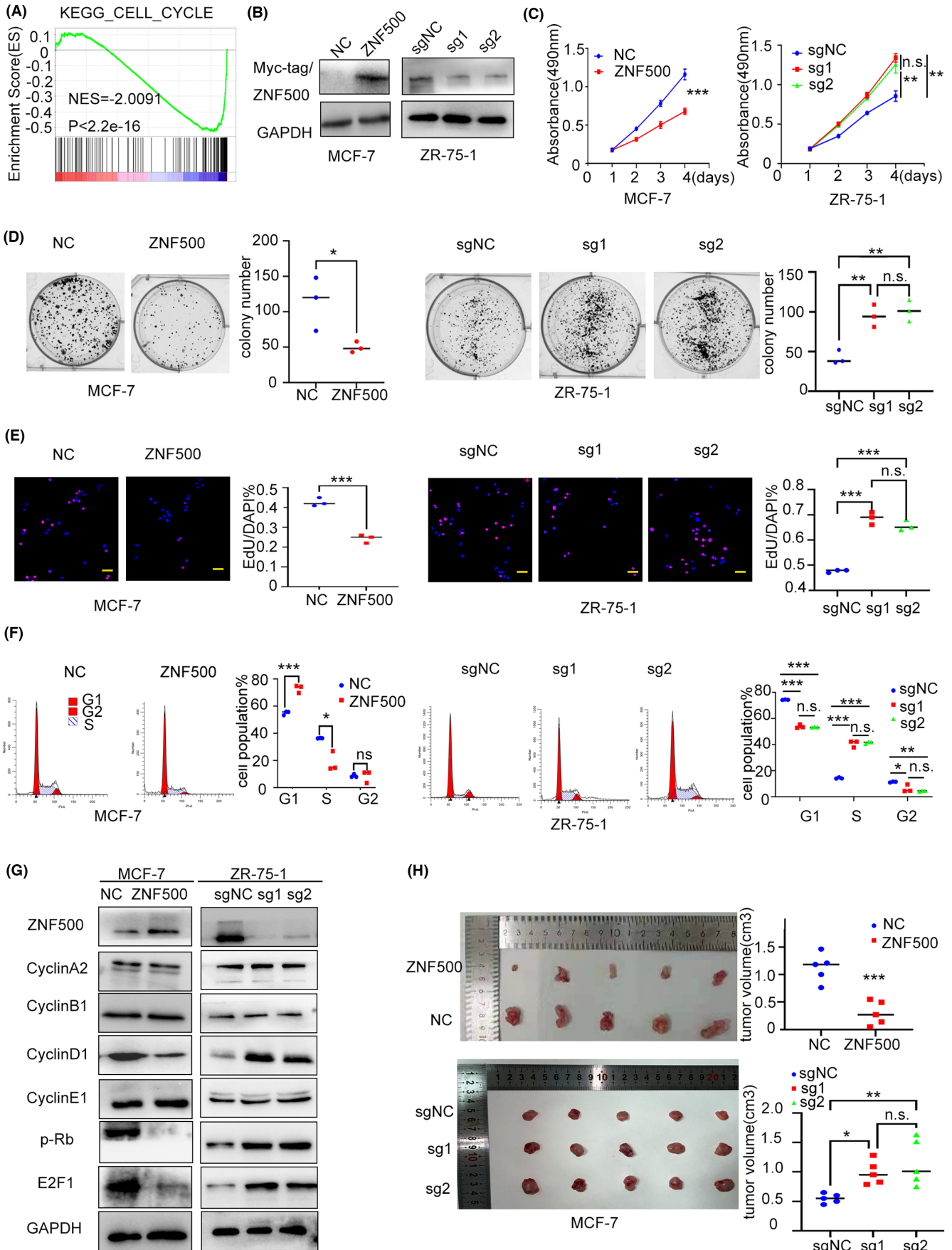
2.11 | RNA microarray

Detailed descriptions are mentioned in the Additional file S1.

2.12 | RNA extraction and real-time PCR

The assays were performed as described in the study by Zhang et al.[19] Primer sequences are shown in Additional file 2: Table S1.

2.13 | GST pull down

The assay was performed as described in the study by Han et al.[21]

2.14 | Statistical analyses

All data were analyzed using SPSS 22.0 (Chicago, IL, USA). The χ2-test was used to evaluate the correlation between ZNF500 expression and clinicopathological factors. All clinicopathological parameters were included in the Cox regression model and assessed by univariate analysis using the enter method and multivariate analysis using the LR method. Student's *t* test was used to analyze differences between two groups. A one-way ANOVA was used to analyze differences among multiple groups. All experiments were performed in triplicate. A *p*-value less than 0.05 was considered statistically significant.

3 | RESULTS

3.1 | ZNF500 level is elevated in breast cancer but negatively correlates with advanced TNM stage, positive lymph node metastasis, and poor prognosis

First, we performed bioinformatic analysis to explore the expression of ZNF500 in human malignancies. According to the Cancer Genome Atlas database pan-cancer analysis, ZNF500 mRNA expression was significantly elevated in most cancerous tissues compared to that in adjacent normal tissues (Figure 1A). We explored its expression specifically in breast cancer and found that ZNF500 mRNA expression was significantly higher in both paired and unpaired breast cancer samples than that in noncancerous samples (Figure 1B and Additional file 3: Figure S1A). We evaluated ZNF500 mRNA expression among breast cancers within different subtypes; ZNF500 displayed the highest expression in luminal A type within the best prognosis and lowest expression in the basal-like type within the worst prognosis (Figure 1C). ZNF500 expression in nontriple-negative breast cancer and nonbasal-like breast cancer patients was significantly higher than that in TNBC or basal-like breast cancer patients (Figure 1D and Additional file 3: Figure S1B). Similarly, ZNF500 expression was significantly higher in ER- or PR-positive breast cancer patients than that in ER- or PR-negative breast cancer patients but visibly lower in HER2-positive breast cancer patients than that in HER2-absent patients (Additional file 3: Figure S1C–E). Moreover, ZNF500 expression was negatively correlated with advanced Scarff–Bloom Richardson (SBR) grading[22] and high Nottingham prognostic Index (NPI) scores[23] (Figures 1E,F). The receiver operating characteristic curve drawn based on ZNF500 levels demonstrated that ZNF500 might be an effective indicator of better prognosis (area under curve=0.634, Additional file 3: Figure S1F). Kaplan–Meier analysis revealed that the OS time of patients with high ZNF500 expression was significantly longer than that of patients with negative expression (Figure 1G). Accordingly, the risk score curve also indicated that the survival time and survival rate of breast cancer patients with high ZNF500 expression were considerably higher than those of patients with low ZNF500 expression (Figure 1H). Univariate Cox regression analysis suggested that ZNF500 could be considered an independent risk prognostic factor for patients with breast cancer (Additional file 3: Figure S1G). ZNF500 expression in patients with WT p53 was significantly higher than that in patients with mutated p53 tissues at DNA, mRNA, and protein levels (Figure 1I and Additional file 3: Figure S1H–I).

Western blot analysis of 12 fresh breast cancer tissues and paired adjacent normal tissues revealed that ZNF500 protein levels were significantly higher in breast cancer tissues than those in noncancerous tissues (*p*=0.0089, Figure 1J and Additional file 3: Figure S1J). Subsequent immunohistochemical staining of 157 breast cancer samples and 61 normal breast tissue samples indicated

FIGURE 3 ZNF500 inhibits P53 ubiquitination and activates P53-P21-E2F4 signal. (A) PCR-array was used to explore DEGs in process of cell cycle within ectopic ZNF500 in MCF-7 cells (B) GEPIA database analysis showed the correlation of mRNA levels between ZNF500 and CDKN1A as well as E2F4 in breast cancer cells. (C, D) qPCR assay was used to detect the mRNA of P21, E2F4 and P53 after overexpressing or knocking out ZNF500 in MCF-7 or ZR-75-1cells. (E) Western blotting was assessed to examine the expression of P53, phosphorylated P53 in Serine 15, P21, CDK4, and E2F4 after ZNF500 overexpression or knockout in MCF-7 or ZR-75-1cells. (F). Western blotting was used to detect the expression of P21 and CyclinD1 in MCF-7 cells after overexpressing ZNF500 together with knocking down P53 by siRNA in MCF-7 cells. (G) MTT, (H) Colony formation assays were performed to test the effect on proliferation of breast cancer cells (I) After being treated with CHX (20uM) at indicated time point, the expression of p53 was detected by western blotting after overexpression of ZNF500 in MCF-7 and ZR-75-1 cells. Western blot assay (J) and immunofluorescence assay (K) were used to detect distribution of P53 in both cytoplasm and nucleus when ZNF500 was overexpressed in MCF-7 cells. (L) The ubiquitination level of P53 was detected by western blotting when ZNF500 was overexpressed. Quantitative data were expressed as the mean±SD of three independent experiments. **$p<0.01$, ***$p<0.001$, t test for two groups and one-way ANOVA for multiple groups, scale bar=10μm.
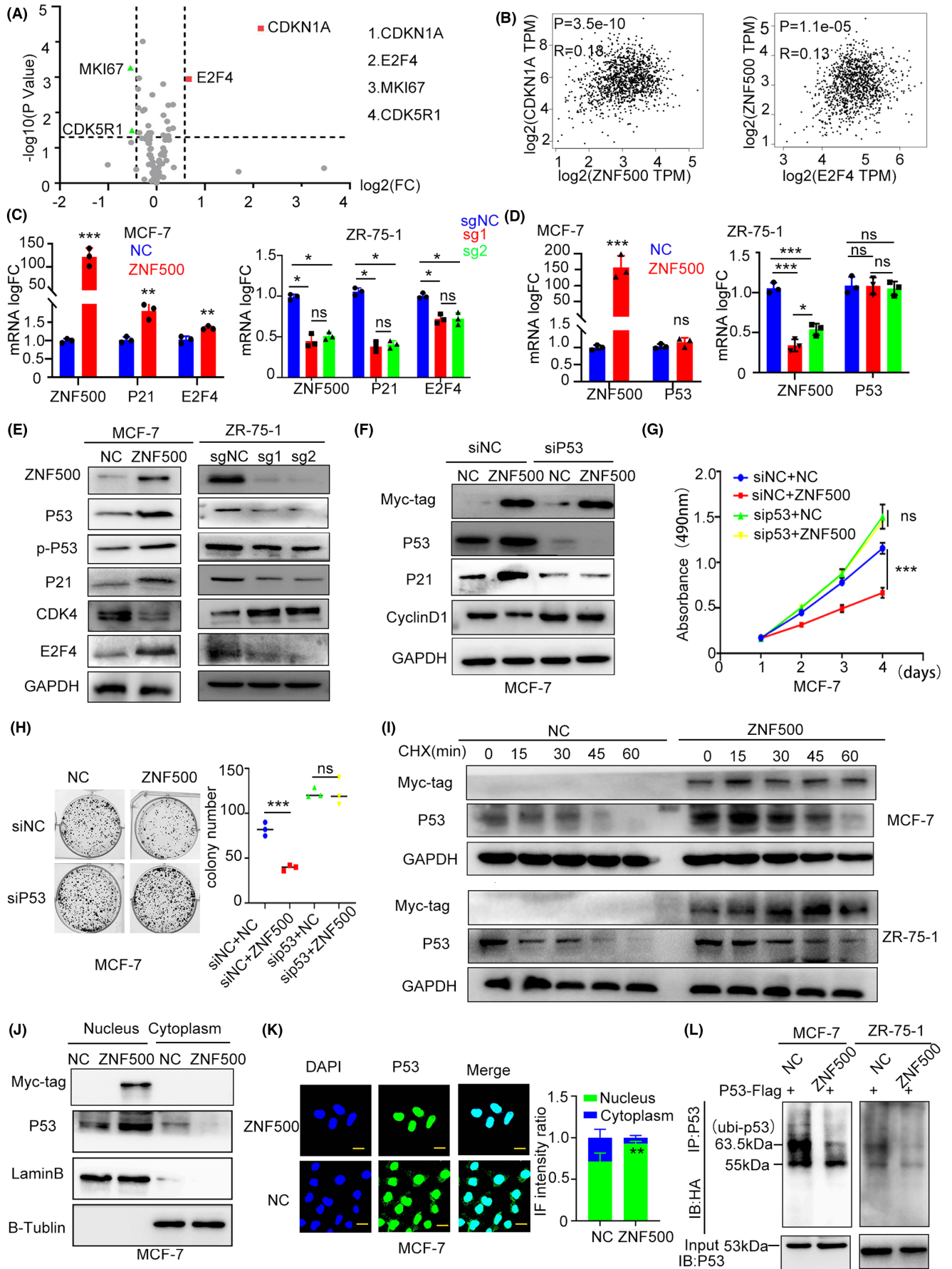
that ZNF500 was highly expressed in the nucleus of breast cancer cells with dim cytosolic expression, and a positive rate of ZNF500 (59.2%, 93/157) in breast cancer was a significantly higher than that in normal breast tissue (10%, 6/61, $p < 0.01$, Figure 1K–N). Statistical analysis indicated that ZNF500 expression was negatively correlated with p53 mutation ($p = 0.001$), TNBC ($p = 0.0013$), advanced TNM stage ($p = 0.018$), and lymph node metastasis ($p = 0.014$, Table 1). Kaplan–Meier analysis revealed that the OS of breast cancer patients with high ZNF500 expression (141.571 ± 3.203) was significantly longer than that of patients with negative ZNF500 expression (121.197 ± 5.847, $p = 0.001$, Figure 1O). Cox univariate and multivariate analyses revealed that, together with advanced TNM stage, ZNF500 expression could be considered an independent prognostic factor for breast cancer ($p = 0.006$, Table 2). We explored ZNF500 expression in diverse breast cancer cell lines and found that ZNF500 expression was higher in cells with p53-WT (MCF-7, ZR75-1, MDA-MB-361, and MDA-MB-175VII) than that in p53-mutant cells (SK-BR-3, MDA-MB-231, and BT549). However, ZNF500 showed increased expression in MDA-MB-453, a p53-null cell line (Figure 1P). Subsequent IF assays indicated that ZNF500 was mainly localized in the nucleus of these cells (Figure 1Q; Additional file 3: Figure S1K).

3.2 | ZNF500 suppresses cell proliferation and induces cell cycle arrest in p53-WT breast cancer cells both in vitro and in vivo

GSEA revealed that DEGs with low ZNF500 expression were closely enriched in the cell cycle process (Figure 2A and Additional file 3: Figure S2A). We overexpressed ZNF500 and knocked it out in several breast cancer cell lines with diverse p53 status (p53 WT cell lines: MCF-7, ZR-75-1, and MDA-MB-175VII; p53 mutant cell lines: SK-BR-3 and MDA-MB-231; and p53-null cell line: MDA-MB-453) using CRISPR-Cas9 guided by two different sgRNAs (Figure 2B and Additional file 3: Figure S3A–C). The MTT assay, colony formation assay, and EdU assay results indicated that proliferation in p53-WT cells was abrogated by overexpression or enhanced by the silencing of ZNF500 (Figure 2C–E and Additional file 3: Figure S3D–F); however, no significant changes were observed in the p53-mutant and p53-null cells (Additional file 3: Figure S3G–L). Therefore, p53-WT cells were selected for subsequent analysis.

We further explored the effects of ZNF500 expression on cell cycle progression using flow cytometry. As shown in Figure 2F and Additional file 3: Figure S4A, ZNF500 overexpression may induce cell cycle arrest in the G1 phase and shorten the S phase. Accordingly, the G1 phase was shortened, and the S phase was prolonged when ZNF500 was knocked out. Western blotting was performed to examine the key factors involved in the cell cycle. The results showed that ZNF500 overexpression or knockout resulted in significantly downregulated or upregulated CyclinD1 expression, respectively. Phosphorylated Rb and E2F1, two downstream effectors of CyclinD1/CDK4, were also decreased or increased upon ectopic or silenced ZNF500. Expression of the other cyclins did not show any changes (Figure 2G and Additional file 3: Figure S4B). We also performed a xenograft assay to explore the effect of ZNF500 expression on cell proliferation in vivo and found that the tumor volume was decreased or increased in ectopic or silenced ZNF500, respectively (Figure 2H).

3.3 | ZNF500 prevents ubiquitination of p53 and activates the p53-p21-E2F4 signaling axis

We performed an RNA-array assay on 90 crucial target genes related to the cell cycle after overexpressing ZNF500. We found that the expression levels of two genes were upregulated (p21 and E2F4) and those of two genes were downregulated (CDK5R1 and MKI67) (Figure 3A and Additional file 3: Figure S5A). The GEPIA database was used to assess the correlation between ZNF500 and the target genes, which indicated that ZNF500 was positively correlated with p21 and E2F4 expression but not with CDK5R1 and MKI67 expression (Figure 3B and Additional file 3: Figure S5B). qPCR results confirmed that p21 and E2F4 mRNA expression was significantly elevated or decreased after overexpression or knockout of ZNF500, respectively (Figure 3C and Additional file 3: Figure S5C). Both p21 and E2F4 are classical downstream target genes of p53 signaling.[24,25] Therefore, we subsequently investigated whether the inhibition of the cell cycle induced by overexpression of ZNF500 is dependent on p53. Both p53 mRNA and protein levels were examined in ectopic or silenced ZNF500 cells, which indicated that p53 mRNA levels remained unaltered. The levels of p53 protein, phosphorylated p53 at Ser15, p21, and E2F4, were significantly enhanced or suppressed, whereas the expression of CDK4 was significantly decreased or

FIGURE 4 ZNF500 directly binds to P53 C-terminal domain through its C2H2 domain to inhibit the proliferation of breast cancer cells. (A, B) Co-IP assay was used to explore the interaction between endogenous and exogenous ZNF500 and P53. (C) GST pull-down assay was used to assess the binding between ZNF500 and P53. (D, E) Representative images showed that ZNF500 and P53 were co-localized in the nucleus by performing IF assay. (F, G) Schematic diagram diverse splicing plasmids for both ZNF500 and P53. (H–J) Co-IP and GST pull-down were used to detect the detailed domains responsible for binding between ZNf500 and P53. (K, L) The ubiquitination level of P53, and protein levels of P21, E2F4 and P53 after transfection with ZNF500-Fl and ZNF500-△C2H2 plasmids by western blotting. (M) Colony formation (N) MTT, (O) Xenografts assays were assessed to detect the effects on cell proliferation with overexpressing ZNF500-Fl, ZNF500-△C2H2 and control both in vitro and in vivo. Quantitative data were expressed as mean ± SD of three independent experiments. **$p < 0.01$, ***$p < 0.001$. t test for two groups and one-way ANOVA for multiple groups. FL, full length; N,N-terminal, DBD, DNA binding domain; C, end C. Scale bar = 10 μm.
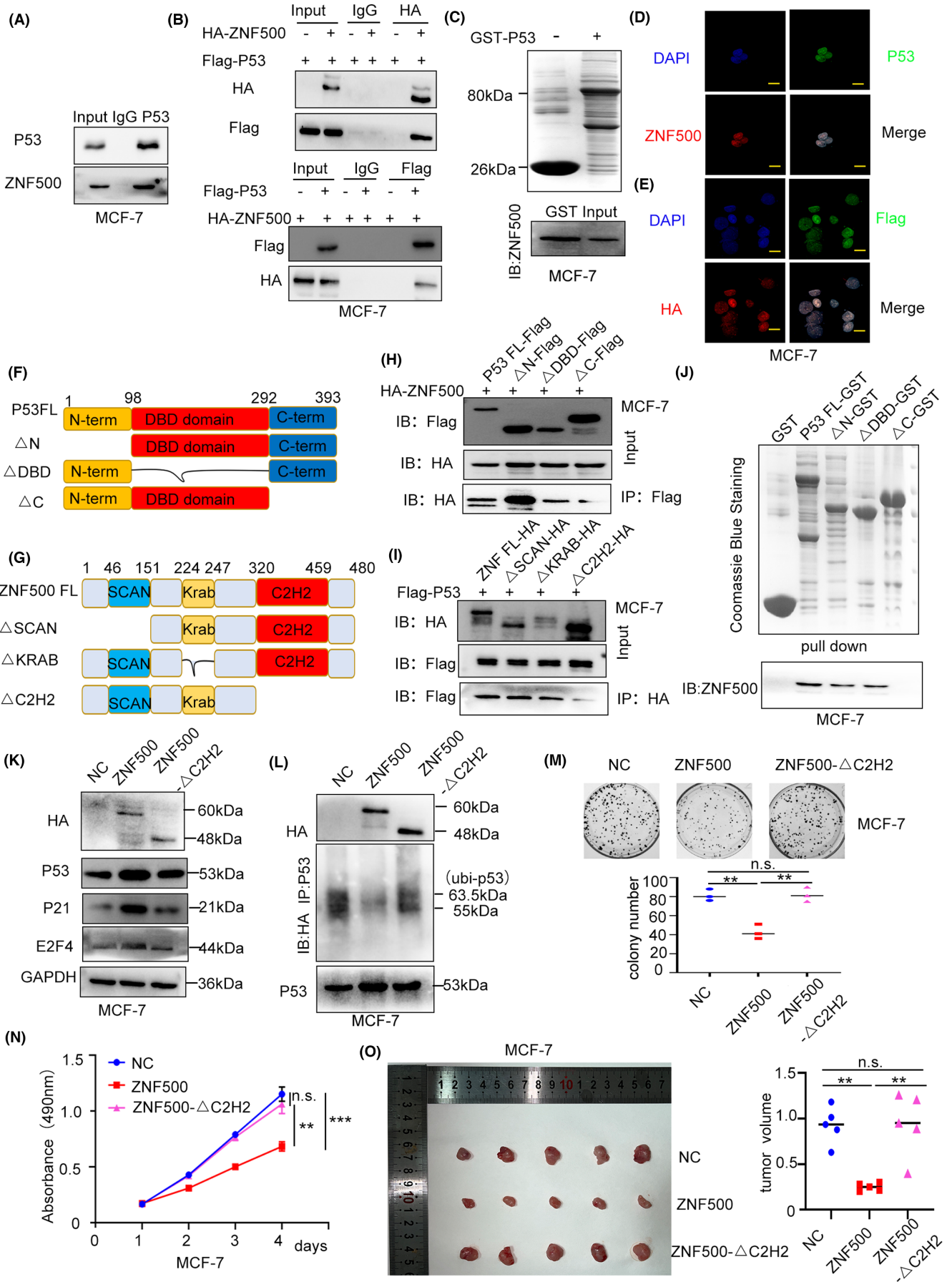
increased after overexpressing or deleting ZNF500 (Figure 3D,E and Additional file 3: Figure S5D,E).

Then, we co-transfected ZNF500 overexpressing plasmid and p53 siRNA as well as the relative control, and the results indicated that upregulation of p21 expression and down-regulation of CyclinD1 expression were counteracted by p53 knockdown (Figure 3F). Moreover, breast cancer cell proliferation was no longer suppressed (Figure 3G,H). The addition of CHX to block de novo protein synthesis showed that the degradation of p53 was significantly delayed after ZNF500 overexpression in MCF-7 and ZR-75-1 cells (Figure 3I). Subsequent WB and IF assays also revealed that overexpression of ZNF500 might prevent nuclear export, a process essential for p53 stability (Figure 3J,K). ZNF500 may be involved in the proteasome process, as indicated by the GSEA (Additional file 3: Figure S2A and S6A). We found that the elevation of p53 expression after ZNF500 overexpression was neutralized by the addition of MG132 for 24h, a proteasome inhibitor (Additional file 3: Figure S6B). Furthermore, overexpression of ZNF500 significantly reduced the ubiquitination of p53 (Figure 3L).

3.4 | ZNF500 directly binds to the C-terminal of p53 via its C2H2 domain

We performed a co-IP assay to examine the interaction between ZNF500 and p53. Our results indicated endogenous and exogenous interaction of ZNF500 with p53 (Figure 4A,B). GST pull-down assay revealed that ZNF500 may directly bind to p53 (Figure 4C). Subsequent IF assays revealed that both endogenous and exogenous p53 and ZNF500 were co-localized in the nucleus of breast cancer cells (Figure 4D,E). Then, we mapped the detailed domain responsible for the binding between ZNF500 and p53 and synthesized a series of splicing mutant plasmids for ZNF500 and p53 (Figure 4F,G). The co-IP assay results indicated that deletion of the C2H2 domain in ZNF500 and the C-terminal domain of p53 may abolish the interaction between ZNF500 and p53 (Figure 4H,I). The GST pull-down results also indicated that ZNF500 is directly bound to the C-terminal domain of p53 (Figure 4J). We then overexpressed ZNF500-full length (FL), ZNF500-△C2H2, and NC plasmids in MCF-7 cells. The WB assay results revealed that overexpression of ZNF500-△C2H2 no longer upregulated expression of p53 and its downstream factors, p21 and E2F4, compared to ZNF500-FL overexpression (Figure 4K). Ubiquitination of p53, as well as cell proliferation, were also not decreased or abrogated after overexpression of ZNF500-△C2H2 (Figure 4L–N). The xenograft assay also confirmed the effect of overexpression of ZNF500-△C2H2 in vivo (Figure 4O).

## 3.5 | ZNF500 binds and stabilizes p53 in a manner that is competitive to MDM2

Our study revealed that ZNF500 binds and stabilizes p53 by preventing its ubiquitination, although ZNF500 is not an E3 ubiquitin ligase. Bioinformatics analysis revealed a negative correlation between ZNF500 expression and the IC50 of nutlin-3a, an MDM2-specific inhibitor (Additional file 3: Figure S7A). We knocked out ZNF500 and added nutlin-3a for 24h and found that suppression of p53 expression induced by silencing ZNF500 at least partially counteracted proliferation (Additional file 3: Figure S7B,C). We speculated that ZNF500 may stabilize p53 by modulating MDM2. A subsequent co-IP assay revealed that endogenous ZNF500, MDM2, and p53 could form a ternary complex (Figure 5A). However, the IF and WB assay results suggested that overexpression of ZNF500 did not affect the expression of MDM2 or its subcellular localization. (Figure 5B,C). Previous studies have indicated that most ubiquitin sites are localized in the C-terminal domain,[26] and MDM2 can also bind to the C-terminal of p53.[27] We speculated whether ZNF500 might compete against MDM2 for the binding to p53, thus stabilizing it. We overexpressed p53 and MDM2 with increasing doses of ZNF500 in MCF-7 cells and performed a co-IP assay, which revealed that the binding between MDM2 and p53 was dose-dependently downregulated by increasing ZNF500 expression (Figure 5D). Similarly, the interaction between ZNF500 and p53 decreased in a dose-dependent manner when MDM2 was overexpressed (Figure 5E).
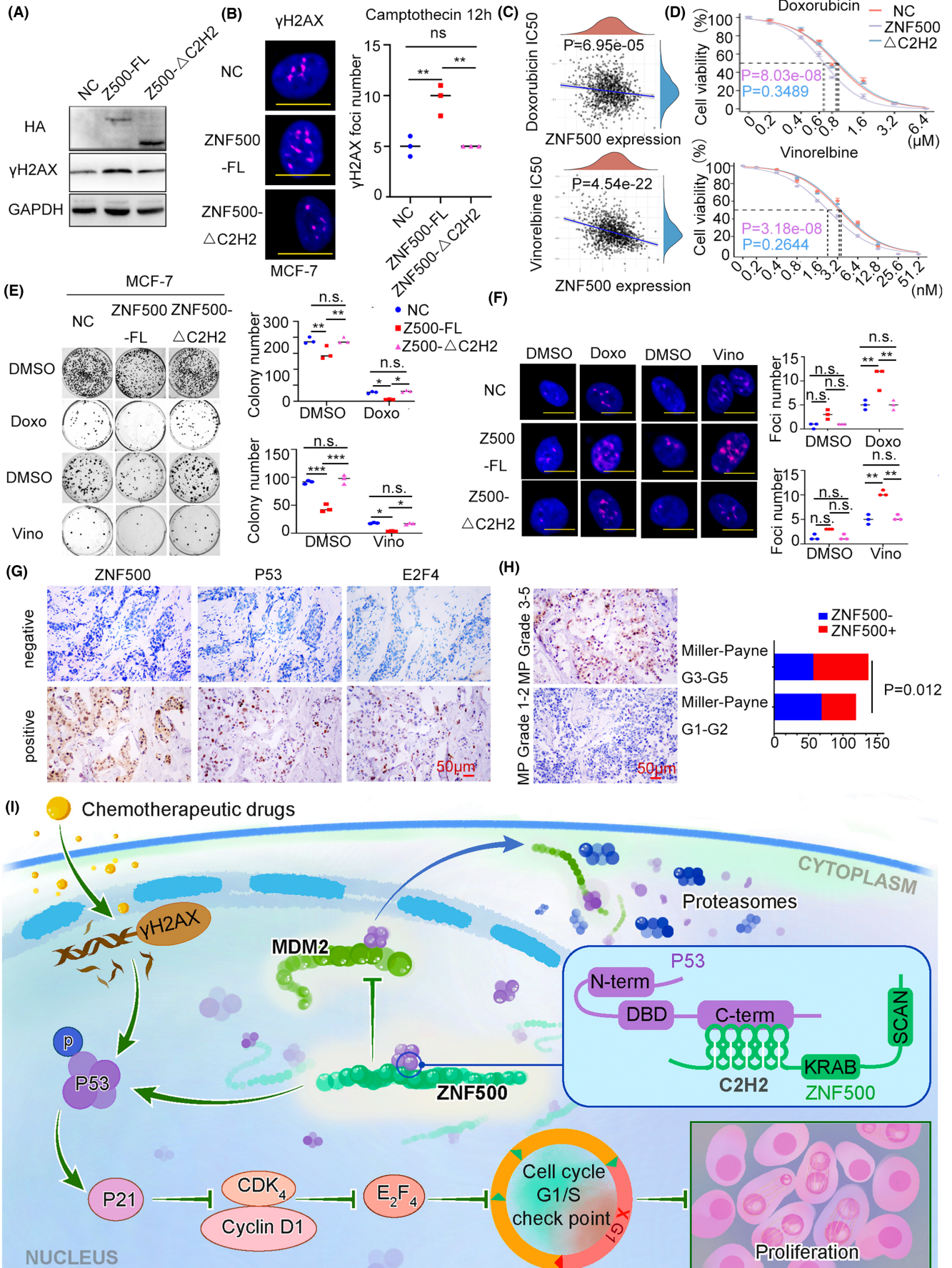
To further explore whether competitive binding to p53 between ZNF500 and MDM2 occurs under physiological conditions, a co-IP assay was performed between endogenous ZNF500 and p53 with increasing doses of MDM2. The results suggested that the endogenous interaction between ZNF500 and p53 was suppressed in a dose-dependent manner (Figure 5F). The endogenous interaction between MDM2 and p53 was also suppressed in a dose-dependent manner in ectopic ZNF500 (Figure 5G). Finally, we overexpressed ZNF500-FL, ZNF500-△C2H2, and the NC at different doses, and the co-IP assay results indicated that overexpression of ZNF500-FL, rather than ZNF500-△C2H2, could disrupt the interaction between MDM2 and p53 (Figure 5H).

3.6 | ZNF500 accelerates DNA damage and sensitizes breast cancer cells to chemotherapy

Previous studies have demonstrated that p53 plays a crucial role in the process of DNA damage.[28] We added camptothecin for 4h to induce DNA damage and found that the overexpression of ZNF500 may strengthen DNA damage, which was revealed by the upregulation of γ-H2AX expression, the DNA damage maker, as well as its nuclear foci (Additional file 3: Figure S8A,B). Furthermore, compared with overexpression of ZNF500-FL, ectopic ZNF500-△C2H2 did not cause more DNA damage, as revealed by the expression and nuclear foci of γ-H2AX (Figure 6A,B). Bioinformatic analysis performed to explore the correlation between ZNF500 expression and chemotherapeutic drugs revealed that ZNF500 expression was significantly negatively correlated with resistance to doxorubicin and vinorelbine, two first-line neoadjuvant chemotherapy drugs for breast cancer patients (Figure 6C). Overexpression of ZNF500 visibly reduced the IC50 of doxorubicin and vinorelbine for 24h,
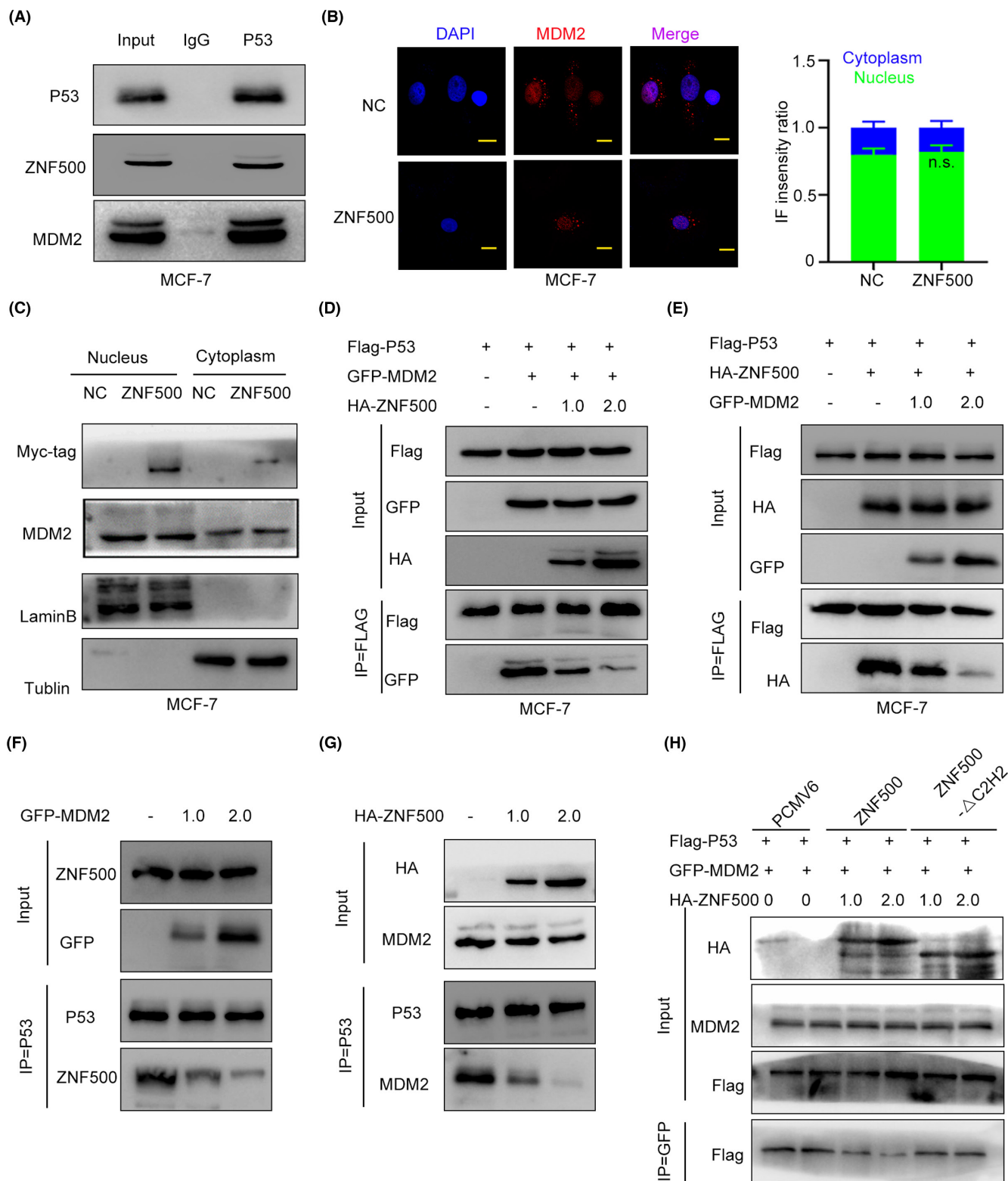
FIGURE 5 ZNF500 and MDM2 competitively bind P53. (A) Co-IP assay was performed to explore the interaction between endogenous ZNF500, MDM2 and P53. (B, C) Western blot and IF assays were used to detect distribution of MDM2 between cytoplasm and nucleus when ZNF500 was overexpressed in MCF-7 cells. (D–G) Co-IP assay was used to evaluate the interaction among MDM2, P53 and ZNF500. (H). Co-IP assay was used to test the interaction between MDM2 and P53 after overexpressing ZNF500-FL, ZNF500-△C2H2 and control, respectively. Quantitative data were expressed as mean±SD of three independent experiments. scale bar = 10μm.

(A)

(B) γH2AX — NC, ZNF500-FL, ZNF500-△C2H2, MCF-7 — Camptothecin 12h

(C) Doxorubicin IC50 P=6.95e-05 ZNF500 expression; Vinorelbine IC50 P=4.54e-22 ZNF500 expression

(D) Doxorubicin P=8.03e-08 P=0.3489; Vinorelbine P=3.18e-08 P=0.2644

(E) MCF-7

(F)

(G) ZNF500, P53, E2F4 — negative, positive — 50μm

(H) Miller-Payne G3-G5, Miller-Payne G1-G2 — ZNF500-, ZNF500+ — P=0.012

(I) Chemotherapeutic drugs

FIGURE 6 ZNF500 promotes DNA damage and enhances neoadjuvant chemotherapy sensitivity. (A) The expression of DNA damage marker γ-H2AX was evaluated by western blotting assay after overexpressing control, ZNF500-FL, ZNF500-△C2H2 in MCF-7 cells within 2 μM CPT for 4 h. (B) Representative IF images of the foci number of γ-H2AX (scale = 10 μm). (C) The correlation between ZNF500 and IC50 for vinorelbine or doxorubicin according to TCGA database. (D) IC50 value was measured after treating MCF-7 with vinorelbine or doxorubicin for 24 h after overexpressing ZNF500. Overexpressing PCMV6, ZNF500-FL, ZNF500-△C2H2 in MCF-7 cells within 0.5 μM doxorubicin or 0.5 nM vinorelbine (E) Colony formation assay was performed to tested the effects on proliferation and (F) Representative IF images of the foci number of γ-H2AX in (scale bar = 10 μm). (G) Representative images of immunohistochemistry staining of ZNF500, P53 and E2F4 in breast cancer patients. Scale bar = 50 μm. Negative staining of ZNF500, P53 and E2F4 were shown in top panel and positive staining were shown in bottom panel (H) Representative images of IHC staining of ZNF500 in breast cancer patients within different Miller-Payne grades. Scale bar = 50 μm. (I) Pathway diagram for ZNF500 action in breast cancer cell lines. Quantitative data were expressed as mean ± SD of three independent experiments. *, $p < 0.05$, **$p < 0.01$, t test for two groups and one-way ANOVA for multiple groups.

TABLE 3 Correlation of ZNF500 with expression of wild-type P53 and E2F4 in 50 breast cancer specimens.

		ZNF500			
		Negative	Positive	r	p
P53	Negative	14	9	0.342	0.022
	Positive	7	19		
E2F4	Negative	16	9	0.436	0.004
	Positive	5	19		

accelerated DNA damage, and abrogated cell proliferation, however, ectopic ZNF500-△C2H2 could not (Figure 6D–F).

Finally, we assessed IHC staining in specimens from 50 breast cancer patients with the p53-WT to evaluate whether the ZNF500–P53–E2F4 axis existed in human breast cancer specimens. The results suggested that ZNF500 was significantly positively correlated with p53 ($p = 0.022$, $r = 0.342$) and E2F4 ($p = 0.004$, $r = 0.436$) expression (Figure 6G, Table 3). We also assessed ZNF500 expression in specimens from patients with diverse therapeutic effects evaluated by Miller/Payne Grades after neoadjuvant chemotherapy. IHC staining results indicated that ZNF500 expression in sensitive patients (Miller/Payne Grade 3–5) was significantly higher than that in resistant patients (Miller/Payne Grade 1–2, $p = 0.012$, Figure 6H).

4 | DISCUSSION

Our studies revealed that ZNF500 was significantly more expressed in the nucleus of breast cancer than normal breast tissues. To explore the reason for ZNF500 upregulation in breast cancer samples, amplification or mutation of ZNF500 were investigated. Using the cBioPortal database (http://www.cbioportal.org/), we determined that there was only 4.22% gene amplification (42/996) and 0.5% mutation (5/996) in all tested specimens. Therefore, gene amplification and mutation are not plausible explanations for elevated ZNF500 levels in breast cancer tissues. Additionally, there was no m6A methylation site localized in ZNF500 (whistleepitranscriptome.com/), which indicated that the mRNA stability of ZNF500 might not be affected by pre-translational modification.

We also tested ZNF500 function in MCF-10A, a normal breast cell, and found that overexpression of ZNF500 still abolished proliferation and activated the P53 signaling pathway axis in MCF-10A cells (Additional file 3: Figure S9). To further confirm the effect on enhanced proliferation induced by ZNF500, two synonymous mutation plasmids of ZNF500 were added back to ZNF500-deficient cells by different sgRNAs. Our results revealed that adding backing ZNF500 might rescue the elevated proliferation induced by a ZNF500 deletion (Additional file 3: Figure S10).

Gu et al. demonstrated that p53 might also transcriptionally increase MDM2 levels in a feedback manner.[29] Therefore, we tested whether p53 transcriptionally upregulated ZNF500 levels in a similar manner; however, overexpression of p53 did not enhance the transcription of ZNF500 (data not shown). Furthermore, Kupers et al. discovered that there is a methylated site in the promoter region of ZNF500.[16] We also found a phosphorylation site (Ser144) in ZNF500. Whether post-transcriptional modifications, such as methylation and phosphorylation of ZNF500, however, overexpression of P53 may not alter the phosphorylation of ZNF500 (Additional file 3: Figure S11).

Overexpression of ZNF500 promoted cell proliferation in p53-WT cells rather than p53-mutated or -null cells, moreover, it upregulated p21 and E2F4, two classical downstream target genes of p53. Next, we further examined the effect on the p53 signaling axis in ectopic ZNF500. We found that overexpression of ZNF500 may dismiss ubiquitination and nuclear export of p53, thus stabilizing it. MDM2 can induce ubiquitin-mediated degradation of p53 via the following three mechanisms: (1) p53 can be degraded directly by MDM2 (2) MDM2 blocks the interaction between p53 and its target genes[30,31]; and (3) binding between MDM2 and p53 may expose the nuclear export site and accelerate its export from the nucleus.[32] Our results are consistent with those of previous studies. Previous studies have also demonstrated that the N-terminal domain of MDM2 mainly binds to the TAD domain (N-terminal) of p53 and promotes its ubiquitination.[33] However, the ubiquitin site was almost exclusively present in the C-terminal domain of p53. Recent studies have also indicated that MDM2 can bind to the C-terminal domain of p53 via its N-terminal.[34] Our results suggest that ZNF500, similar to MDM2, might also bind to the C-terminal of p53 and can inhibit ubiquitin-mediated degradation of p53.
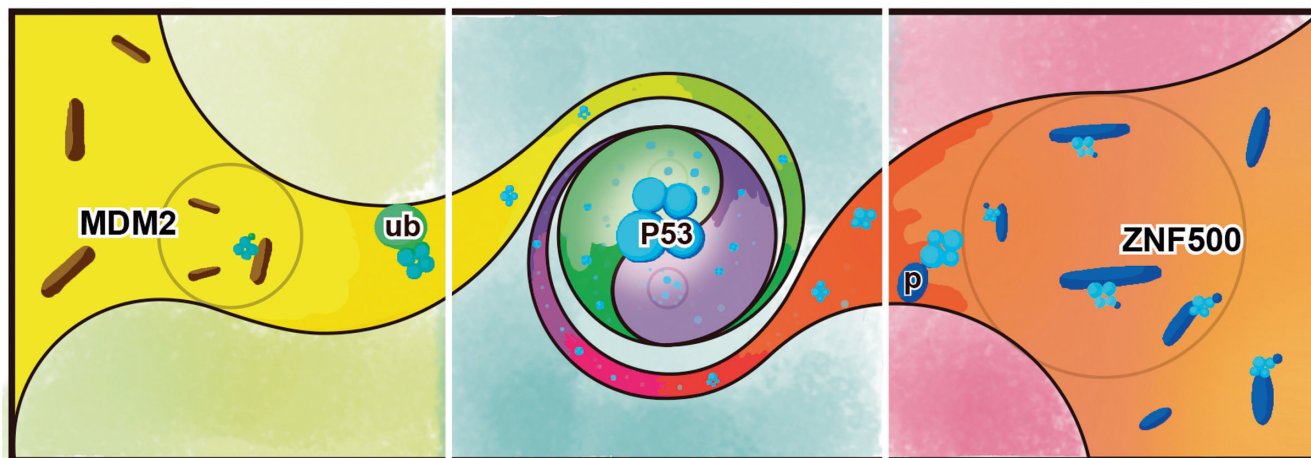
FIGURE 7 Pathway diagram for ZNF500 action in breast cancer cell lines.

We also explored whether mutated P53 could modulate ZNF500. However, overexpression of P53-R270H or P53-S20A might not alter the protein and mRNA level, moreover, the phosphorylation of ZNF500 was also unchanged (Additional file 3: Figure S11). The relationship between mutated P53 and ZNF500 should be further explored in the future.

Our study revealed that ZNF500 can directly bind to the C-terminal of p53 via its C2H2 domain. This interaction may prevent ubiquitin-mediated degradation by MDM2, thus abrogating the proliferation of breast cancer cells, strengthening DNA damage, and sensitizing breast cancer patients to chemotherapy (Figure 6I and Figure 7).

AUTHOR CONTRIBUTIONS

WM, WF and XZ performed study concept and design; WM, YZ and XZ performed development of methodology and writing, review and revision of the paper; BY, YW, RH, JY, KH, YG and XZ provided acquisition, analysis and interpretation of data, and statistical analysis; ND, YJ and CL provided technical and material support. All authors read and approved the final paper.

CONFLICT OF INTEREST STATEMENT

The authors have no conflict of interest.

ETHICS STATEMENT

The study protocol was approved by the Institutional Review Board of China Medical University.

All participants provided written informed consent, and the study was conducted according to the Declaration of Helsinki principles.

Registry and the Registration No. of the study/trial: N/A.

Animal Studies: The animals used in this study were treated according to the National Institutes of Health Guide for the Care and Use of Laboratory Animals (NIH Publications No. 8023, revised 1978).

ORCID

Xiupeng Zhang https://orcid.org/0000-0001-5872-5205

REFERENCES

1. Sung H, Ferlay J, Siegel RL, et al. Global cancer statistics 2020: GLOBOCAN estimates of incidence and mortality worldwide for 36 cancers in 185 countries. *CA Cancer J Clin.* 2021;71(3):209-249.
2. Draganescu M, Carmocan C. Hormone therapy in breast cancer. *Chirurgia (Bucur).* 2017;112(4):413-417.
3. Jacobs AT, Martinez Castaneda-Cruz D, Rose MM, Connelly L. Targeted therapy for breast cancer: an overview of drug classes and outcomes. *Biochem Pharmacol.* 2022;204:115209.
4. Liu Y, Tavana O, Gu W. p53 modifications: exquisite decorations of the powerful guardian. *J Mol Cell Biol.* 2019;11(7):564-577.
5. Williams AB, Schumacher B. p53 in the DNA-Damage-Repair Process. *Cold Spring Harb Perspect Med.* 2016;6(5):a026070.
6. Sionov RV, Haupt Y. Apoptosis by p53: mechanisms, regulation, and clinical implications. *Springer Semin Immunopathol.* 1998;19(3):345-362.
7. Hernandez Borrero LJ, El-Deiry WS. Tumor suppressor p53: biology, signaling pathways, and therapeutic targeting. *Biochim Biophys Acta Rev Cancer.* 2021;1876(1):188556.
8. Duffy MJ, Synnott NC, Crown J. Mutant p53 in breast cancer: potential as a therapeutic target and biomarker. *Breast Cancer Res Treat.* 2018;170(2):213-219.
9. Silwal-Pandit L, Langerod A, Borresen-Dale AL. TP53 mutations in breast and ovarian cancer. *Cold Spring Harb Perspect Med.* 2017;7(1):a026252.
10. Lacroix M, Riscal R, Arena G, Linares LK, Le Cam L. Metabolic functions of the tumor suppressor p53: implications in normal physiology, metabolic disorders, and cancer. *Mol Metab.* 2020;33:2-22.

11. Steegenga WT, van der Eb AJ, Jochemsen AG. How phosphorylation regulates the activity of p53. *J Mol Biol*. 1996;263(2):103-113.

12. Brooks CL, Gu W. The impact of acetylation and deacetylation on the p53 pathway. *Protein Cell*. 2011;2(6):456-462.

13. Brooks CL, Gu W. p53 regulation by ubiquitin. *FEBS Lett*. 2011;585(18):2803-2809.

14. Kon N, Gu W. p53 activation vs. stabilization: an acetylation tale from the C-terminal tail. *Onco Targets Ther*. 2021;8:58-60.

15. Brooks CL, Li M, Gu W. Mechanistic studies of MDM2-mediated ubiquitination in p53 regulation. *J Biol Chem*. 2007;282(31):22804-22815.

16. Kupers LK, Fernandez-Barres S, Mancano G, et al. Maternal dietary glycemic index and glycemic load in pregnancy and offspring cord blood DNA methylation. *Diabetes Care*. 2022;45(8):1822-1832.

17. Deng N, Zhang X, Zhang Y. BAIAP2L1 accelerates breast cancer progression and chemoresistance by activating AKT signaling through binding with ribosomal protein L3. *Cancer Sci*. 2022;114:764-780.

18. Li J, Zhang X, Hou Z, et al. P130cas-FAK interaction is essential for YAP-mediated radioresistance of non-small cell lung cancer. *Cell Death Dis*. 2022;13(9):783.

19. Zhang X, Liu Y, Fan C, et al. Lasp1 promotes malignant phenotype of non-small-cell lung cancer via inducing phosphorylation of FAK-AKT pathway. *Oncotarget*. 2017;8(43):75102-75113.

20. Zhang X, Yu X, Jiang G, et al. Cytosolic TMEM88 promotes invasion and metastasis in lung cancer cells by binding DVLS. *Cancer Res*. 2015;75(21):4527-4537.

21. Han Q, Rong X, Lin X, et al. WBP2 negatively regulates the Hippo pathway by competitively binding to WWC3 with LATS1 to promote non-small cell lung cancer progression. *Cell Death Dis*. 2021;12(4):384.

22. Amat S, Penault-Llorca F, Cure H, et al. Scarff-Bloom-Richardson (SBR) grading: a pleiotropic marker of chemosensitivity in invasive ductal breast carcinomas treated by neoadjuvant chemotherapy. *Int J Oncol*. 2002;20(4):791-796.

23. Ogston KN, Miller ID, Payne S, et al. A new histological grading system to assess response of breast cancers to primary chemotherapy: prognostic significance and survival. *Breast*. 2003;12(5):320-327.

24. Benson EK, Mungamuri SK, Attie O, et al. p53-dependent gene repression through p21 is mediated by recruitment of E2F4 repression complexes. *Oncogene*. 2014;33(30):3959-3969.

25. Taylor WR, Schonthal AH, Galante J, Stark GR. p130/E2F4 binds to and represses the cdc2 promoter in response to p53. *J Biol Chem*. 2001;276(3):1998-2006.

26. Lohrum MA, Woods DB, Ludwig RL, Balint E, Vousden KH. C-terminal ubiquitination of p53 contributes to nuclear export. *Mol Cell Biol*. 2001;21(24):8521-8532.

27. Poyurovsky MV, Katz C, Laptenko O, et al. The C terminus of p53 binds the N-terminal domain of MDM2. *Nat Struct Mol Biol*. 2010;17(8):982-989.

28. Anand SK, Sharma A, Singh N, Kakkar P. Entrenching role of cell cycle checkpoints and autophagy for maintenance of genomic integrity. *DNA Repair (Amst)*. 2020;86:102748.

29. Brooks CL, Gu W. p53 ubiquitination: Mdm2 and beyond. *Mol Cell*. 2006;21(3):307-315.

30. Fischer M. Census and evaluation of p53 target genes. *Oncogene*. 2017;36(28):3943-3956.

31. Kussie PH, Gorina S, Marechal V, et al. Structure of the MDM2 oncoprotein bound to the p53 tumor suppressor transactivation domain. *Science*. 1996;274(5289):948-953.

32. Juven-Gershon T, Oren M. Mdm2: the ups and downs. *Mol Med*. 1999;5(2):71-83.

33. Mendoza M, Mandani G, Momand J. The MDM2 gene family. *Biomol Concepts*. 2014;5(1):9-19.

34. Wong JH, Alfatah M, Sin MF, et al. A yeast two-hybrid system for the screening and characterization of small-molecule inhibitors of protein-protein interactions identifies a novel putative Mdm2-binding site in p53. *BMC Biol*. 2017;15(1):108.

SUPPORTING INFORMATION

Additional supporting information can be found online in the Supporting Information section at the end of this article.